Research Square

Preprints are preliminary reports that have not undergone peer review.
They should not be considered conclusive, used to inform clinical practice,
or referenced by the media as validated information.

Aryl Hydrocarbon Receptor Mediates Resistance to Endocrine Therapy in Breast Cancer Cells through PTEN/AKT Pathway

Ayodele Alaiya
King Faisal Specialist Hospital & Research Centre
Radwan AA
King Saud University
Zakia Shinwari
King Faisal Specialist Hospital & Research Centre
Rabab Allam
King Faisal Specialist Hospital & Research Centre
Falah Al-Mohanna
King Faisal Specialist Hospital & Research Centre
Abdullah Al-Dhfyan
aaldhfyan@kfshrc.edu.sa

King Faisal Specialist Hospital & Research Centre

Research Article

Keywords: Aryl Hydrocarbon Receptor, Endocrine therapy, Resistance

Posted Date: April 19th, 2026

DOI: https://doi.org/10.21203/rs.3.rs-9103920/v1

License: This work is licensed under a Creative Commons Attribution 4.0 International License. Read Full License

Additional Declarations: No competing interests reported.

Abstract

Background

Endocrine therapy is generally the primary treatment option for breast cancer patients whose tumors express estrogen receptor. However, resistance to endocrine therapy is a significant clinical challenge. While the Aryl Hydrocarbon Receptor (AhR) is well established in breast cancer development, its potential role in driving resistance to endocrine treatments remains not fully understood.

Methods

TNMplot tool and Kaplan–Meier Plotter were used to evaluate AhR gene expression and prognostic value in breast cancer patients. The basal and inducible levels of AhR and CYP1A1 in breast cancer and mammary epithelial cell lines were determined by RT-PCR, immunofluorescence, flow cytometry, and western blot analysis. Integrative proteomic analysis study was performed as a tool for comparative expression analysis of human mammary epithelial cells treated by AhR agonist. Additionally, molecular docking study was conducted using AutoDock4.2 software.

Results

In our study, we have shown through analysis of publicly available databases that overexpression of the AhR gene predicts poorer survival in breast cancer patients treated with endocrine therapy. Functional in vitro studies indicate that treatment with Tamoxifen and Fulvestrant activates AhR in breast cancer cell lines. Pharmacological inhibition of AhR sensitizes breast cancer cells to endocrine therapeutic agents and reduces treatment induced side population cells expansion through AKT pathway inhibition. Mechanistically, integrative proteomic analyses demonstrate that AhR activation induces translational upregulation via the mTORC1–p70S6K–eIF4 pathway. Furthermore, inhibition of AhR reduced p70S6K and eIF4 phosphorylation induced by endocrine therapy treatment in breast cancer cells.

Conclusion

Together, our work reveals that AhR is a mediator of endocrine therapy resistance through the AKT/p70S6K–eIF4 axis and presents AhR antagonism as a therapeutic intervention worthy of further preclinical investigation.

Introduction

The aryl hydrocarbon receptor (AhR) is a cytoplasmic transcription factor that plays a major role in regulating cell fate and proliferation. (1, 2) In the cytoplasm, AhR exists in a non-functional form as part of a complex containing heat-shock proteins (HSP90) and AhR inhibitory proteins (AIP).(3, 4) Aryl hydrocarbons, such as 2,3,7,8-tetrachlorodibenzodioxin (TCDD) and 7,12-dimethylbenz[a]anthracene (DMBA), act as agonists of AhR, leading to the dissociation of HSP90 and AIP from the receptor. The free AhR then translocates to the nucleus, where it binds to another nuclear protein called ARNT.(5) The AhR-ARNT complex then binds to a specific DNA recognition sequence known as the xenobiotic response element (XRE) and ultimately activate the expression of its downstream target genes, including CYP1A1 and CYP1B1.(6–8)

Several studies on the carcinogenicity of poly aryl hydrocarbons such as TCDD and DMBA have demonstrated the critical role of CYP1A1 and CYP1B1 gene induction in the metabolic activation of these compounds into their ultimate carcinogenic epoxide and diol-epoxide derivatives.(9) These bioactivated metabolites alkylate DNA and leading to the formation of adducts and mutations. The inability of DMBA to induce tumors in CYP1 knockout mice provides strong evidence supporting the tumorigenic role of AHR downstream target CYP genes.(10)

Chemical carcinogens can impact stem cells properties and this relationship is supported by multiple lines of evidence. Furthermore, treatment of MCF-7 cells with the AhR agonist TCDD resulted in increased the number and size of cancer stem cell (CSC) populations as demonstrated by mammosphere formation assays.(11) Additionally, Aldhfyan et al. demonstrated that the AhR/CYP1A1 signaling axis controls cancer stem cell proliferation and resistance to chemotherapy by modulating the PTEN/AKT and β-catenin signaling pathways.(12)

Breast cancer remains the most frequently diagnosed malignancy in women worldwide, with approximately 70–80% of cases expressing estrogen receptors (ER+).(13) Endocrine therapy is first therapeutic option used primarily in hormone sensitive cancers.(14) The pharmacological effect of this therapy aims to interfere with the hormonal signaling pathways that enabled tumor growth and proliferation.(15) Although endocrine therapy is effective resistance is frequently developed. Making it a major clinical obstacle and driving continued investigation into the underlying molecular mechanisms and potential combination therapies.(16)

The PI3K/AKT signaling pathway plays a critical role in regulating cell growth, survival, and metabolism, and its dysregulation has been strongly associated with resistance to endocrine therapy in breast cancer.(17) Dysregulation of the PI3K/AKT pathway is often observed as over activation, which promotes oncogenic transformation primarily due to

mutations in the PIK3CA gene or loss of tumor suppressors such as PTEN.(18) Activation of the PI3K/AKT pathway enables cancer cells to bypass the requirement for estrogen signaling, promoting their growth and survival.(19)

Since the Aryl Hydrocarbon Receptor (AhR) is a known mediator of breast carcinogenesis, it is highly plausible that it may also contribute to endocrine therapy resistance. Therefore, this study was designed with two primary objectives: first, to investigate the relationship between AhR signaling pathway activation and endocrine therapy resistance. Second, to provide a scientific rationale for the potential use of AhR antagonists in combination with endocrine therapy to enhance treatment response and prevent resistance.

Material and Methods

Chemical carcinogens were obtained from Toronto Laboratories Research (Toronto, Canada). Dulbecco's Modified Eagle's Medium (DMEM) and TRIzol reagent were purchased from Invitrogen. The High Capacity cDNA Reverse Transcription Kit and SYBR® Green PCR Master Mix were obtained from Applied Biosystems (Foster City, CA). Nitrocellulose membranes were purchased from Bio-Rad Laboratories (Hercules, CA). Primary antibodies against target proteins and HRP-conjugated secondary antibodies were purchased from Santa Cruz Biotechnology, Inc. (Santa Cruz, CA). Western blot detection kits and Enhanced Chemiluminescence (ECL) reagents were obtained from Amersham Biosciences (Piscataway, NJ).

Cell Culture

Human cancer cell lines MCF-7 and T47D, and human mammary epithelial cells (HMLE) (American Type Culture Collection, Rockville, MD), were cultured in DMEM supplemented with 10% fetal bovine serum, 200 µM L-glutamine, and 2% antibiotic–antimycotic mixture (ABM) (GIBCO).

Side population

For the characterization of cancer stem cells (CSCs), the side population (SP) technique was employed. Briefly, 1×10^6 cells/mL were suspended in DMEM in FACS tubes. Cells were then incubated with DyeCycle Violet (DCV; Invitrogen Molecular Probes) at a final concentration of 10 µM. All analyses were performed using a LSRFortessa flow cytometer (BD Biosciences).

Determination of the protein expression

Total protein lysates were extracted and protein concentrations were determined using the Lowry method with bovine serum albumin as the standard. Expression of PTEN (Invitrogen,), p-Akt1 (Thr 308) (Santa Cruz), Phospho-p70 S6 Kinase (Thr389, Thr412) (Invitrogen) were assessed by Western blot analysis using specific antibodies and results normalized to the endogenous reference protein GAPDH (Santa Cruz). Bands were visualized using enhanced chemiluminescence.

Therapy resistance

Resistance to endocrine therapy is a hallmark feature of cancer stem cells (CSCs). To evaluate whether the AhR/CYP1A1 pathway mediates CSC resistance to endocrine therapy, cancer cells were pretreated for 4 hours with the AhR antagonist α-naphthoflavone (α-NF) at a concentration of 500 nM. Subsequently, the cells were exposed to varying doses of endocrine therapeutic agents: Tamoxifen (TAM) at 10 and 20 μM, and Fulvestrant (FUL) at 50 and 100 nM. After 48 hours of incubation, cells were stained with DyeCycle Violet (DCV) for side population (SP) cell analysis.

RNA isolation and real-time PCR (RT-PCR)

Total RNA was extracted using TRIzol reagent (Invitrogen®) according to the manufacturer's instructions. RNA quality was maintained at a 260/280-absorbance ratio of ~ 2.0 OD as described previously.(20) The cDNA was synthesized, and the mRNA expression of target genes was quantified using human primers CYP1A1 (F: CTATCTGGGCTGTGG GCAA and R: CTGGCTCAAGCACAACTTGG), and β-ACTIN (F: TATTGGCAACGAGCGGTTCC and R: GGCATAGAGGTCTTTACGGATGTC) using 7500 Real-Time PCR System (Life Technologies Co., Grand Island, NY). The mRNA expression levels of target genes in all samples were calculated using the ΔΔ CT method.(21)

Immunofluorescence assay

MCF-7, T47D, and HMLE cells were treated with the test drugs for the indicated time intervals. Following treatment, cells were plated on glass slides at a density of 20,000 cells/cm and cultured for 3 days before being fixed in 4% formaldehyde. Fixed cells were then stained with primary antibodies against AhR (Invitrogen), PTEN (Cell Signalling), Phospho-Akt (Ser473) (Cell Signaling) Phospho-p70 S6 Kinase (Thr389, Thr412) (Invitrogen), Phospho-eIF4E (Ser209) (Invitrogen) followed by Alexa Fluor 594-conjugated secondary antibodies (Invitrogen). Nuclear DNA was counterstained with 1 μg/mL 4′,6-diamidino-2-phenylindole (DAPI). Each sample was stained in triplicate for each antibody. Fluorescence intensity and intracellular localization were analyzed using a BD Pathway 855 Bioimager (San Jose, CA).

Molecular Docking Study

For molecular docking studies, The tamoxifen structure, with the lowest energy levels, and the crystal structures of the aryl hydrocarbon receptor-aryl hydrocarbon receptor nuclear translocator (AHR-ARNT) complexd with tapinarof (pdb id: 8XS6) were prepared (22). After mixing the nonpolar hydrogen atoms with AutoDock4.2 tools and saving them in pdbqt format, the Autodock4.2 parameters, the Lamarckian genetic approach, the polar hydrogen atoms, and the Kollman charges were found.(23) The ligand was made to be flexible, while the protein was made to be stiff. An autoGrid grid box that covered the binding site of the tapinarof-xray structure was set up with a size of 25 X 25 X 25 Å, a grid spacing of 0.5 Å, and coordinate centres at X = -16, Y = -7.0, and Z = 0.0. We made ten docked conformations with a tolerance of two for root mean square deviation (RMSD).

Protein in solution-digestion and Protein identification by mass spectrometry: LC-MS Analysis

A one-dimensional Nano Acquity liquid chromatography coupled with tandem mass spectrometry on Synapt G2 (Waters, Manchester, UK) was used to generate label-free expression proteomics data based on both qualitative and quantitative protein changes between the samples as previously described (Alkhayal 2023). Briefly, Detectors set up using 2ng/µL Leucine Enkephalin (556.277 Da), Mass (m/z) calibration was achieved on a separate infusion of 500 fmol [Glu] 1-Fibrinopeptide B (GluFib, 785.843 Da), using the Mass Lynx IntelliStart. Other parameters include capillary voltage 3.5 Kv, sample cone 50 V, extraction cone 5V, source temperature 85°C, cone gas 10L/h, Nano flow gas 0.3 bar and purge gas 800 L/h. All analyses were done on Trizaic Nano source (Waters, Manchester, UK) ionization in the positive ion mobility mode.(24) Proteomic experiments were conducted using HMLE (human mammary luminal epithelial) cells to investigate protein-level changes upon AhR activation. Cells were treated with 10 µM DMBA for 48 hours, after which whole-cell protein extraction was performed. The extracted protein samples were then analyzed using the Synapt G2 mass spectrometry platform. Progenesis QI for Proteomics (QIfP), version 3.0 (Waters/Nonlinear Dynamics), was used for automated data processing and database searching. Differential protein expression between samples was assessed as previously described. (25, 26) Proteins displaying statistically significant changes (ANOVA, $P \leq 0.05$) and at least a 1.5 difference in expression were considered differentially expressed.

Kaplan–Meier Overall Survival Analysis

The Kaplan–Meier Plotter (kmplot.com, accessed on 20 April 2025) is a robust, web-based tool for performing real-time survival analysis, integrating gene expression and clinical

data from GEO, EGA, TCGA, and other repositories using Kaplan–Meier plots alongside Cox proportional hazards modeling. In this study, we analyzed a cohort of 2,976 breast cancer patients from the Kaplan–Meier Plotter database. Patients were stratified into high- and low-expression groups based on the median mRNA expression of the AhR gene. Kaplan–Meier survival curves for overall survival (OS) were generated, and corresponding hazard ratios (HRs), 95% confidence intervals (CIs), and log-rank p-values to assess prognostic significance were computed.

Statistical Analysis

Data are expressed as mean ± standard error of the mean (SEM). Comparative analyses were performed using an unpaired two-tailed Student's t-test in GraphPad Prism 10 (GraphPad Software, San Diego, CA). Statistical significance was determined as follows*$P < 0.05$; **$P < 0.01$; ***$P < 0.001$,****$P < 0.0001$; and ns denotes not significant.

Results

AhR gene expression predict worse overall survival in breast cancer patients treated with endocrine therapy

We initially aimed to evaluate the clinical predictive value of AhR gene expression in breast cancer patients by analyzing publicly available clinical data. Our findings, utilizing the TNMplot tool, indicate that AhR gene expression and it downstream target CYP1B1 but not CYP1A1 (data not show) are significantly elevated in tumor and metastatic tissues compared to normal breast tissues, as shown in Fig. 1a. The differential expression of the aryl hydrocarbon receptor (AhR) between tumor and adjacent normal tissues underscores the necessity to assess its prognostic value in overall survival analyses using Kaplan-Meier Plotter RNA sequence database. Elevated expression of the AhR correlates with reduced overall survival in breast cancer patients, as demonstrated by Kaplan–Meier survival analyses. This association was particularly pronounced in patients with lymph node metastasis, as shown in Fig. 1b. Elevated expression of the AhR correlates with reduced overall survival (OS) in breast cancer patients who are positive for both lymph node metastasis and estrogen receptor expression, particularly among those undergoing endocrine therapy. The observed predictive value of AhR gene expression in endocrine therapy underscores the necessity to evaluate whether treatment with endocrine therapeutic agents in vitro induces activation of the AhR.

Endocrine therapeutics agents Tamoxifen (TAM) and Fulvestrant (FUL) induced AHR nuclear translocation and increased CYP1A1 gene expression

We sought to investigate the potential link between endocrine therapy and resistance mechanisms by assess the pharmacological impact of two widely used endocrine therapeutic agents TAM and FUL on the activation of AhR *in vitro*. Treatment of MCF-7 and T47D breast cancer cells with both agents induced nuclear translocation of AhR, as demonstrated by immunofluorescence assays. Furthermore, a significantly increased expression of the AhR downstream target gene CYP1A1 was measured by RT-PCR. In MCF-7 cells, treatment with TAM (1 µM) inhibited nuclear translocation of the AhR and suppressed expression of CYP1A1 gene expression. Conversely, treatment with a higher dose of TAM (10 µM) for 48 hours induced significant nuclear localization of AhR and upregulated CYP1A1 gene expression by approximately 23-fold compared to untreated controls, as shown in Fig. 2a and d. These findings suggest that tamoxifen modulates the AhR as a mixed agonist/antagonist, exhibiting dose-dependent effects on AhR activation. In contrast, FUL activated AhR signaling in tested doses at nanomolar concentrations, as evidenced by nuclear translocation of AhR and a ≥ 10-fold induction of CYP1A1 gene expression compared to untreated controls. These data suggest distinct modes of action between TAM and FUL in their interaction with the AhR. To gained insight a structural basis for tamoxifen's interaction with AhR, docking study was undertaken using Autodock4.2 program. For validating our docking procedure the bound x-ray ligand (A1LWH, topinarof) was re-docked inside AHR active site. The docking pose of TAM, compared with that of the topinrof, X-rary structure, is shown in Fig. 2d. TAM showed same orientation of topinrof inside the binding site and adopts the same position as the tapinarof x-ray structure. Additionally, it is oriented similarly inside the hydrophobic pockets of the active site. TAM showed significant estimated binding energy (E = -8.06 kcal/mol) and inhibition constant (Ki = 156.27 nM) compared to those of tapinarof (E = -10.65 kcal/mol, Ki = 15.52 nM). Furthermore, the results revealed that TAM is less potent than tapinarof. The interaction of binding conformations of TAM to AhR binding site as illustrated in Fig. 2e, showed absence of hydrogen bond interactions. TAM exhibited hydrophobic interactions with the aromatic rings and hydrocarbon side chains of several amino acid residues lining the AhR binding site, including HIS289.B, PHE293.B, GLY319.B, TYR320.B, ILE323.B, TYR334.B, SER344.B, ILE347.B, PHE349.B, LEU351.B, SER363.B, ALA365.B, ALA379.B, and GLN381.B. The docking results suggest that tamoxifen can occupy the AhR ligand-binding domain with a moderate binding affinity supporting previous experimental observations of AhR modulation by TAM.(27, 28)

AhR inhibition increased therapeutic effect of Tamoxifen and Fulvestrant in breast cancer cells

The interaction of TAM and FUL on AhR may suggests potential crosstalk influencing therapy resistance. To investigate this hypothesis, we aimed to evaluate the impact of pharmacological inhibition of AhR on resistance to TAM and FUL in breast cancer cells. Our findings indicate that inhibition of the AhR using α-NF (500 nM) potentiated the anti-

proliferative effects of TAM in breast cancer cell line MCF-7 as shown in Fig. 3a and in T47D cells in supplementary Fig. 1a. However, treatment with α-NF and FUL did not exhibit significant synergistic effects. Mechanistically, analysis of cell cycle progression revealed that inhibition of the AhR using α-NF (500 nM) induced G1-phase cell cycle arrest in MCF-7 cells. Treatment with TAM and α-NF resulted in a more G1 arrest compared to TAM treatment alone as shown in Fig. 3b. In contrast, treatment with FUL and α-NF did not significantly alter cell cycle progression, which may explain the absence of synergistic effects on cell proliferation between FUL and AhR inhibition. To evaluate whether the cell cycle arrest will lead eventually to cell death, we assess the impact of AhR inhibition on apoptosis using Annexin V staining by flow cytometry. Our results demonstrate that combined treatment in MCF-7 cells significantly enhanced apoptotic cell death compared to TAM and FUL alone treatments as shown in Fig. 3c and d. Same observation was detected in T47D cells as shown in supplementary Fig. 1b. Our findings indicated that AhR inhibition potentiate the effects of endocrine therapies in breast cancer cells.

AhR inhibition enhances the reduction of side population induced by Tamoxifen and Fulvestrant treatment through PTEN/AKT pathway

Therapy resistance in breast cancer cells may rely on the presence and behavior of breast cancer stem cells (BCSCs).(29) Several markers that can be used to characterized and isolated these cells. One of which is the side population (SP) phenotype, defined by their capacity to efflux fluorescent dye. This efflux mechanism results in a distinct low-fluorescence profile detectable by flow cytometry.(30) SP cells have been shown to exhibit stem cell-like properties, including enhanced clonogenicity, tumorigenicity, and resistance to chemotherapy.(31, 32) Therefore, we aimed to assess the impact of AhR inhibition on the expansion of side population (SP) cells in breast cancer before and after treatment with TAM and FUL. Treatment of MCF-7 cells with TAM and FUL at varying concentrations demonstrated differential effects on the side population (SP) cells. However, treatment with both agents and α-NF significantly reduced the SP cell percentage by over 80% compared to untreated cells as shown in Fig. 4a and b. Of note, α-NF alone inhibited SP cells percentage, suggesting AhR activity is required for SP cells maintenance. While TAM treatment alone resulted in a decrease in SP cells, FUL treatment resulted in increased in SP cells expansion. Phosphatase and tensin homolog (PTEN), a key tumor suppressor, has been found to regulate the side population (SP) phenotype in cancer stem-like cells by modulating the phosphoinositide 3-kinase (PI3K)/AKT signaling pathway.(33) Therefore, we sought to study the impact of AhR inhibition on PTEN/AKT pathway by evaluate the expression of PTEN and AKT phosphorylation using immunofluorescence and western blotting techniques. Treatment of MCF-7 cells with TAM (10 μM) and FUL (50 nM) increased PTEN protein expression, as shown by immunofluorescence in Fig. 4e. This effect was further enhanced by combined

treatment with α-NF. In contrast, TAM and FUL treatment alone reduced AKT phosphorylation and combined treatment led to a greater inhibition of AKT phosphorylation. Western blotting analysis revealed that treatment of MCF-7 cells with TAM and FUL slightly increased AKT phosphorylation levels. However, this increase was suppressed by α-NF alone or in combination with TAM and FUL. Unlike the PTEN expression levels observed by immunofluorescence, western blotting showed that PTEN was upregulated by FUL treatment but not by TAM alone. Notably, a further increase in PTEN expression was detected in TAM and α-NF. These findings indicate that AhR activity is required for SP expansion under treatment stress through PTEN/AKT pathway.

Proteomic Analysis of Human Mammary Epithelial Cells Treated with AhR agonist DMBA, revealed regulation of eIF4 and p70S6K Signaling pathway.

The effect of AhR inhibition on central signaling nodes such as the AKT pathway, which regulates numerous downstream target proteins, prompted us to evaluate the impact of AhR activation on the global cellular proteome. We employed a quantitative label-free nanoLC-MS-based approach to identify downstream targets with potential relevance for biomarker discovery for breast cancer. To investigate protein changes potentially contributing to breast carcinogenesis, we utilized normal human mammary epithelial cells (HMLE) treated with AHR agonist DMBA in (10 μM) as our *in vitro* model system. Global proteomic profiling of HMLE cells following AhR activation identified 1,506 unique protein species across all sample groups. Comparative analysis between DMBA-treated (DMBA-T) and control (DMBA-Ctrl) cells revealed 242 significantly differentially expressed proteins (DEPs) (ANOVA $p < 0.05$, fold change ≥ 1.5). These DEPs were subsequently subjected to functional enrichment analysis using the Qiagen Ingenuity Pathway Analysis (IPA) platform to identify perturbed canonical pathways, upstream regulators, and causal networks associated with AhR activation. Integration of canonical pathway enrichment, causal network analysis, and known AhR signaling demonstrates that endocrine therapy induces AhR-driven translational activation through mTORC1–p70S6K–eIF4 signaling. Causal regulators (EGFR, MYC, LARP1, IGF2BP, TXNIP) and networks involving NF-κB, HSP90, and PI3K–AKT reveal a coordinated stress adaptation response that maintains protein synthesis and survival during therapeutic pressure. Functionally, this positions AhR as a master upstream node linking xenobiotic sensing and metabolic stress to translational reprogramming and drug resistance in ER+ breast cancer cells. The graphical representations of the canonical pathways and the top five causal networks are described in Fig. 5a. Collectively, these modules converge on AhR–mTORC1–eIF4/p70S6K signaling, leading to enhanced translation, metabolic adaptation, and cell survival. This integrated feedback loop underlies endocrine therapy resistance by sustaining anabolic and stress-response pathways despite estrogen-receptor blockade. Schematic summarizes the major molecular interactions linking AhR activation to translational reprogramming is shown in Fig. 6b. The major molecular interactions included Inflammation (orange): TNF–

NF-κB–associated inflammatory signaling promotes stress adaptation and pro-survival cytokine responses. Transcriptional stress (beige): The HSP90–p38 MAPK–RNA polymerase II module links proteotoxic and transcriptional stress responses to AhR activation. mTOR/ translation signaling (blue): mTOR–AKT–p70S6K drives phosphorylation of eIF4/eIF2 and enhances cap-dependent translation and protein synthesis. RNA regulation/proteasome (green): PI3K–ERK–Proteasome signaling supports sustained mRNA processing and degradation of misfolded proteins. Proteostasis and RNA-binding control (light green): IGF2BP, EIF2A, and FUS regulate mRNA stability and translation initiation.

AhR activation is required for endocrine therapy to induced phosphorylation of p70S6K and eIF4

To confirm the involvement of these pathways in AhR activation in HMLE cells, we assessed the phosphorylation of eIF4 and p70S6K induced by two different AhR agonists, TCDD and DMBA, using an immunofluorescence assay. Treatment of HMLE cells with TCDD (10 nM) and DMBA (10 µM) for 48 hours resulted in a marked increase in the phosphorylation of both eIF4 and p70S6K compared to untreated cells as shown in Fig. 6a. To link endocrine therapy and eIF4 and p70S6K activation, we sought to evaluate the phosphorylation status of both proteins in MCF-7 breast cancer cells treated with FUL and TAM. As expected, endocrine therapeutic agents induced the phosphorylation of both proteins in MCF-7 cells. Inhibition of AhR significantly reduced the expression of therapy induced phosphorylation of eIF4 and p70S6K as shown in Fig. 6b. Furthermore, Immunoblotting assay showed that AhR inhibition by α-NF treatment significantly suppressed p70S6K phosphorylation and further suppression was detected in combined treatment of TAM at 10 and 20µM. Next, we aimed to evaluate the clinical predictive value of the correspondence gene expression of eIF4 and p70S6K in breast cancer patients by analyzing publicly available clinical data. Our findings, utilizing the TNMplot tool, indicate that RPS6KB1 gene expression but not EIF4E3 significantly elevated in tumor and metastatic tissues compared to normal breast tissues, as shown in Fig. 6c. Furthermore, we aimed to evaluate the clinical predictive value of correspondence EIF4E3 and RPS6KB1 gene expression in breast cancer patients by analyzing overall survival (OS) using the Kaplan-Meier Plotter RNA-seq database, and to determine whether these genes serve as predictive markers for patients receiving endocrine therapy. Kaplan–Meier survival analyses demonstrated that elevated expression of EIF4E3 and RPS6KB1 is significantly associated with reduced OS in both the general breast cancer cohort and in ER-positive (ER+) patients. More importantly, increased expression of both genes correlates with reduced OS in breast cancer patients treated with endocrine therapy as shown in Fig. 6d. These data indicated that elevated expression of EIF4E3 and RPS6KB1 may serve as potential biomarkers for poor prognosis and endocrine therapy resistance in breast cancer patients.

Discussion

Emerging evidence indicates that a ligand-activated transcription factor AhR may play a role in endocrine therapy resistance in breast cancer. Activation of AhR has been associated with the upregulation of drug metabolizing enzymes and transporters enabling efflux of therapeutic agents and may reduce drug efficacy.(34) Conversely, inhibition of AhR has been resulted in reduce the percentage of $ALDH^+$ cells in tamoxifen resistant breast cancer cells.(35) Therefore, a possible crosstalk between AhR signaling and endocrine therapy resistance development may take a place. Furthermore, exploring the effects of AhR inhibition on endocrine therapy response and resistance could provide valuable insights into the mechanisms underlying treatment failure and identify novel therapeutic targets and combinations. This study aimed first to evaluate the clinical predictive value of AhR gene expression in breast cancer patients. Using the TNMplot tool, we found that AhR expression is significantly elevated in both tumor and metastatic breast tissues compared to normal tissue. Furthermore, we evaluated the prognostic significance of AhR expression by performing overall survival (OS) analysis using the Kaplan–Meier Plotter RNA-seq database. Kaplan–Meier survival analysis demonstrated that high AhR expression correlates with reduced overall survival (OS) in breast cancer patients. Further stratification showed that this correlation is particularly strong in patients whose tumors are estrogen receptor (ER)-positive with lymph node positive and those undergoing endocrine therapy. These findings indicated that AhR may serve as prognostic marker for tumor development and endocrine therapy resistance in breast cancer patients.

On cellular level, we have shown direct interaction between endocrine therapeutic agents and the AhR signaling pathway. Through examined the effect of two well-known endocrine agents TAM and FUL, immunofluorescence assay revealed that TAM at a low concentration (1 µM) inhibited AhR translocation into the nucleus, whereas treatment with a higher concentration (10 µM) in MCF-7 and T47D cell lines resulted in increased nuclear accumulation of AhR. In contrast, FUL treatment at both 1 and 10 (nM) concentrations induced AhR nuclear translocation in these cell lines. These findings suggest that TAM and FUL interact with AhR via different mode of action. TAM act as an AhR antagonist at low concentrations but in higher concentration act like an agonist. On the other hand, FUL consistently promotes AhR activation. These findings were validated by measuring the gene expression of the AhR downstream target, CYP1A1. Consistent with the AhR nuclear localization, treatment of MCF-7 cells with TAM at 1 µM for 48 hours led to inhibition of CYP1A1 gene expression. In contrast, a higher concentration of TAM (10 µM) caused about 22-fold increase in CYP1A1 expression compared to untreated cells. As expected, treatment with FUL at 1 and 10 (nM) concentrations induced CYP1A1 gene expression by about 11 fold and 13 fold, respectively. We reasoned the difference in the mode of action between TAM and FUL on AhR activity to the nature of interactions of these drugs with

their primary target, the estrogen receptor (ER). While TAM acts as a selective estrogen receptor modulator (SERM), FUL acts as a selective estrogen receptor degrader (SERD). (36, 37)

The activation of AhR by TAM and FUL suggests a crosstalk that may contribute to endocrine therapy resistance. To explore this hypothesis, we aimed to evaluate whether pharmacological inhibition of AhR could interfere with endocrine therapy resistance in breast cancer cells. Additionally, we employed cell proliferation assay, DNA cell cycle profiling, and apoptosis detection to evaluate the impact of AhR inhibition on cellular response. We demonstrated that pretreatment of MCF-7 cells with the AhR antagonist α-NF at 500 (nM) sensitized the cells to TAM induced inhibition of cell proliferation, compared to treatment with TAM alone. However, only modest effects were observed in combination with FUL. Consistent with cell proliferation assay, DNA cell cycle analysis showed that AhR inhibition enhanced TAM induced accumulation of cells at the G1 checkpoint, while no significant effect was observed with FUL treatment. Of note, treatment with α-NF alone induced accumulation of cells at the G1 checkpoint. Our data on DNA cell cycle analysis are consistent with previous report showing that inhibition of the AhR downstream target CYP1A1 gene impacts cell cycle progression.(38) More importantly, sensitization to apoptosis induction was observed with both agents in MCF-7 and T47D cells.

Several reports have demonstrated that AhR regulates cancer stem cell (CSC) proliferation, maintenance, and chemoresistance in breast cancer cells.(12, 39) However, whether endocrine therapy resistance induced by AhR activation is mediated through CSCs expansion remains not fully understood. In this study, we demonstrated that pharmacological inhibition of AhR significantly reduced the percentage of side population (SP) cells in both TAM and FUL treated breast cancer cells. Mechanistically, we have shown that pharmacological inhibition of AhR increased the expression of the tumor suppressor gene PTEN in MCF-7 cells treated with TAM and FUL. This upregulation of PTEN protein was confirmed using immunofluorescence and Western blotting. Consistent with the PTEN induction, a significant reduction in phosphorylated AKT levels was observed. These findings consistence with our previous report on the regulation of the PTEN/AKT pathway by AhR activation.(12) Furthermore, similar inhibition of phosphorylated AKT was also reported with AhR antagonist Resveratrol.(40)

The AKT pathway regulates protein synthesis via phosphorylates p70S6K and 4E-BP1 through mTORC1. Phosphorylation of p70S6K enhances ribosomal protein S6 activity and promoting translation. On the other hand, phosphorylation of 4E-BP1 releases eIF4E enabling initiate cap-dependent translation.(41, 42). With this context, we have shown using proteomic analysis of HMLE cells treated with the AhR agonist DMBA (10 µM) for 48hrs that eIF4 and p70S6K signaling pathways are among the most significantly affected

pathway ($p = 0.000024$). This suggests a strong link between AhR activation and the regulation of protein synthesis process through modulation of the AKT/mTOR axis. Independently, we validate these findings, by treatment of HMLE cells with two widely used AhR agonists, TCDD and DMBA, and we have shown that treatment led to increased phosphorylation of both eIF4 and p70S6K. Furthermore, we have shown that AhR activity is required for eIF4 and p70S6K phosphorylation under TAM and FUL treatment. Additionally our work support the previous reports on the involvement of eIF4 and p70S6K in endocrine therapy resistance.(43, 44) Furthermore, we analyzed clinical predictive value of correspondence EIF4E3 and RPS6KB1 gene expression in breast cancer patients. We have shown that elevated expression of EIF4E3 and RPS6KB1 is significantly associated with reduced overall survival in both the general breast cancer cohort and in ER-positive patients. Notably, increased expression of these genes also correlates with poorer overall survival specifically in breast cancer patients receiving endocrine therapy. These findings are consistent with previous reports highlighting the clinical predictive value of EIF4E3 and RPS6KB1 in breast cancer patients and support our findings.(43, 45)

Conclusion

Overall, this work showed that AhR inhibition reduced endocrine therapy resistance through activation of PTEN and subsequent inhibition of AKT pathway. Our proteomic analysis of HMLE cells treated with DMBA, indicates a crosstalk between AhR activation and the regulation of protein synthesis through induced phosphorylation of both eIF4 and p70S6K. Further preclinical investigations are warranted to evaluate the efficacy of combining AhR antagonists with endocrine therapy for prevent the development of therapy resistance in breast cancer.

Declarations

Data availability

Data are available upon written request to the study corresponding author.

Acknowledgements

The authors would like to thank Mr. Amer Almzroua for his assistance with side population experiments using the LSRFortessa flow cytometer.

Funding

This study was supported by King Faisal Specialist Hospital and Research Center Grant no. RAC 2240045, Riyadh, Kingdom of Saudi Arabia.

Author information

Authors and Affiliations

King Faisal Specialist Hospital & Research Centre, Riyadh, 11211, Kingdom of Saudi Arabia.

Ayodele Alaiya, Zakia Shinwari , Rabab Allam , Falah Al-Mohanna , Abdullah Al-Dhfyan

College of Pharmacy, King Saud University, Riyadh, Saudi Arabia

Radwan AA

Contributions

AA: Contributed to data collection, run, analysis, interpretation of proteomics data, and edited the manuscript. AR: Collected and analyzed/Interpreted data (docking study).FM, RA and ZS: Collected and analyzed/Interpreted data. AD: Designed the study, supervised data collection and analysis, interpreted the findings, and wrote the manuscript. All authors reviewed and approved the manuscript prior to submission.

Corresponding Author

Abdullah Al Dhfyan, Research Laboratories Department, King Faisal Specialist Hospital & Research Centre, Riyadh, 11211, Kingdom of Saudi Arabia.

Electronic address: aaldhfyan@kfshrc.edu.sa

Ethics declarations

Not applicable.

Consent for publication

Not applicable.

Competing interests

The authors declare no competing interests.

References

1. Kerzee JK, Ramos KS. Constitutive and inducible expression of Cyp1a1 and Cyp1b1 in vascular smooth muscle cells: role of the Ahr bHLH/PAS transcription factor. Circ Res. 2001;89(7):573–82.
2. Whitelaw ML, Gottlicher M, Gustafsson JA, Poellinger L. Definition of a novel ligand binding domain of a nuclear bHLH receptor: co-localization of ligand and hsp90

binding activities within the regulable inactivation domain of the dioxin receptor. EMBO J. 1993;12(11):4169–79.

3. Sogawa K, Fujii-Kuriyama Y. Ah receptor, a novel ligand-activated transcription factor. J Biochem. 1997;122(6):1075–9.
4. Denison MS, Vella LM, Okey AB. Structure and function of the Ah receptor for 2,3,7,8-tetrachlorodibenzo-p-dioxin. Species difference in molecular properties of the receptors from mouse and rat hepatic cytosols. J Biol Chem. 1986;261(9):3987–95.
5. Hankinson O. The aryl hydrocarbon receptor complex. Annu Rev Pharmacol Toxicol. 1995;35:307–40.
6. Moore M, Narasimhan TR, Steinberg MA, Wang X, Safe S. Potentiation of CYP1A1 gene expression in MCF-7 human breast cancer cells cotreated with 2,3,7,8-tetrachlorodibenzo-p-dioxin and 12-O-tetradecanoylphorbol-13-acetate. Arch Biochem Biophys. 1993;305(2):483–8.
7. Pollenz RS. The mechanism of AH receptor protein down-regulation (degradation) and its impact on AH receptor-mediated gene regulation. Chem Biol Interact. 2002;141(1–2):41–61.
8. Whitlock JP. Jr. Induction of cytochrome P4501A1. Annu Rev Pharmacol Toxicol. 1999;39:103–25.
9. Shimada T, Fujii-Kuriyama Y. Metabolic activation of polycyclic aromatic hydrocarbons to carcinogens by cytochromes P450 1A1 and 1B1. Cancer Sci. 2004;95(1):1–6.
10. Buters JT, Sakai S, Richter T, Pineau T, Alexander DL, Savas U, et al. Cytochrome P450 CYP1B1 determines susceptibility to 7, 12-dimethylbenz[a]anthracene-induced lymphomas. Proc Natl Acad Sci U S A. 1999;96(5):1977–82.
11. Jung JW, Park SB, Lee SJ, Seo MS, Trosko JE, Kang KS. Metformin represses self-renewal of the human breast carcinoma stem cells via inhibition of estrogen receptor-mediated OCT4 expression. PLoS ONE. 2011;6(11):e28068.
12. Al-Dhfyan A, Alhoshani A, Korashy HM. Aryl hydrocarbon receptor/cytochrome P450 1A1 pathway mediates breast cancer stem cells expansion through PTEN inhibition and beta-Catenin and Akt activation. Mol Cancer. 2017;16(1):14.
13. Early Breast Cancer Trialists', Collaborative G. Effects of chemotherapy and hormonal therapy for early breast cancer on recurrence and 15-year survival: an overview of the randomised trials. Lancet. 2005;365(9472):1687–717.
14. Osborne CK, Schiff R. Mechanisms of endocrine resistance in breast cancer. Annu Rev Med. 2011;62:233–47.
15. Clarke R, Leonessa F, Welch JN, Skaar TC. Cellular and molecular pharmacology of antiestrogen action and resistance. Pharmacol Rev. 2001;53(1):25–71.
16. Johnston SR. Enhancing Endocrine Therapy for Hormone Receptor-Positive Advanced Breast Cancer: Cotargeting Signaling Pathways. J Natl Cancer Inst. 2015;107(10).

17. Mayer IA, Arteaga CL. The PI3K/AKT Pathway as a Target for Cancer Treatment. Annu Rev Med. 2016;67:11–28.
18. Samuels Y, Waldman T. Oncogenic mutations of PIK3CA in human cancers. Curr Top Microbiol Immunol. 2010;347:21–41.
19. Miller TW, Rexer BN, Garrett JT, Arteaga CL. Mutations in the phosphatidylinositol 3-kinase pathway: role in tumor progression and therapeutic implications in breast cancer. Breast Cancer Res. 2011;13(6):224.
20. Al-Dhfyan A, Alaiya A, Al-Mohanna F, Attwa MW, AlAsmari AF, Bakheet SA, et al. Crosstalk between aryl hydrocarbon receptor (AhR) and BCL-2 pathways suggests the use of AhR antagonist to maintain normal differentiation state of mammary epithelial cells during BCL-2 inhibition therapy. J Adv Res. 2023;50:177–92.
21. Livak KJ, Schmittgen TD. Analysis of relative gene expression data using real-time quantitative PCR and the 2(-Delta Delta C(T)) Method. Methods. 2001;25(4):402–8.
22. Diao X, Shang Q, Guo M, Huang Y, Zhang M, Chen X, et al. Structural basis for the ligand-dependent activation of heterodimeric AHR-ARNT complex. Nat Commun. 2025;16(1):1282.
23. Morris GM, Huey R, Lindstrom W, Sanner MF, Belew RK, Goodsell DS, et al. AutoDock4 and AutoDockTools4: Automated docking with selective receptor flexibility. J Comput Chem. 2009;30(16):2785–91.
24. Alkhayal Z, Shinwari Z, Gaafar A, Alaiya A. Fluconazole-Induced Protein Changes in Osteogenic and Immune Metabolic Pathways of Dental Pulp Mesenchymal Stem Cells of Osteopetrosis Patients. Int J Mol Sci. 2023;24(18).
25. Colak D, Alaiya AA, Kaya N, Muiya NP, AlHarazi O, Shinwari Z, et al. Integrated Left Ventricular Global Transcriptome and Proteome Profiling in Human End-Stage Dilated Cardiomyopathy. PLoS ONE. 2016;11(10):e0162669.
26. Alaiya AA, Aljurf M, Shinwari Z, Almohareb F, Malhan H, Alzahrani H, et al. Protein signatures as potential surrogate biomarkers for stratification and prediction of treatment response in chronic myeloid leukemia patients. Int J Oncol. 2016;49(3):913–33.
27. DuSell CD, Nelson ER, Wittmann BM, Fretz JA, Kazmin D, Thomas RS, et al. Regulation of aryl hydrocarbon receptor function by selective estrogen receptor modulators. Mol Endocrinol. 2010;24(1):33–46.
28. Jin UH, Lee SO, Safe S. Aryl hydrocarbon receptor (AHR)-active pharmaceuticals are selective AHR modulators in MDA-MB-468 and BT474 breast cancer cells. J Pharmacol Exp Ther. 2012;343(2):333–41.
29. Bai X, Ni J, Beretov J, Graham P, Li Y. Cancer stem cell in breast cancer therapeutic resistance. Cancer Treat Rev. 2018;69:152–63.

30. Goodell MA, Brose K, Paradis G, Conner AS, Mulligan RC. Isolation and functional properties of murine hematopoietic stem cells that are replicating in vivo. J Exp Med. 1996;183(4):1797–806.
31. Hirschmann-Jax C, Foster AE, Wulf GG, Nuchtern JG, Jax TW, Gobel U, et al. A distinct side population of cells with high drug efflux capacity in human tumor cells. Proc Natl Acad Sci U S A. 2004;101(39):14228–33.
32. Kondo T, Setoguchi T, Taga T. Persistence of a small subpopulation of cancer stem-like cells in the C6 glioma cell line. Proc Natl Acad Sci U S A. 2004;101(3):781–6.
33. Bleau AM, Hambardzumyan D, Ozawa T, Fomchenko EI, Huse JT, Brennan CW, et al. PTEN/PI3K/Akt pathway regulates the side population phenotype and ABCG2 activity in glioma tumor stem-like cells. Cell Stem Cell. 2009;4(3):226–35.
34. Ramadoss P, Marcus C, Perdew GH. Role of the aryl hydrocarbon receptor in drug metabolism. Expert Opin Drug Metab Toxicol. 2005;1(1):9–21.
35. Dubrovska A, Hartung A, Bouchez LC, Walker JR, Reddy VA, Cho CY, et al. CXCR4 activation maintains a stem cell population in tamoxifen-resistant breast cancer cells through AhR signalling. Br J Cancer. 2012;107(1):43–52.
36. Jordan VC. Chemoprevention of breast cancer with selective oestrogen-receptor modulators. Nat Rev Cancer. 2007;7(1):46–53.
37. Nathan MR, Schmid P. A Review of Fulvestrant in Breast Cancer. Oncol Ther. 2017;5(1):17–29.
38. Rodriguez M, Potter DA. CYP1A1 regulates breast cancer proliferation and survival. Mol Cancer Res. 2013;11(7):780–92.
39. Stanford EA, Wang Z, Novikov O, Mulas F, Landesman-Bollag E, Monti S, et al. The role of the aryl hydrocarbon receptor in the development of cells with the molecular and functional characteristics of cancer stem-like cells. BMC Biol. 2016;14:20.
40. Jiang H, Shang X, Wu H, Gautam SC, Al-Holou S, Li C, et al. Resveratrol downregulates PI3K/Akt/mTOR signaling pathways in human U251 glioma cells. J Exp Ther Oncol. 2009;8(1):25–33.
41. Manning BD, Toker A. AKT/PKB Signaling: Navigating the Network. Cell. 2017;169(3):381–405.
42. Saxton RA, Sabatini DM. mTOR Signaling in Growth, Metabolism, and Disease. Cell. 2017;169(2):361–71.
43. Miller TW, Hennessy BT, Gonzalez-Angulo AM, Fox EM, Mills GB, Chen H, et al. Hyperactivation of phosphatidylinositol-3 kinase promotes escape from hormone dependence in estrogen receptor-positive human breast cancer. J Clin Invest. 2010;120(7):2406–13.
44. Mamane Y, Petroulakis E, Rong L, Yoshida K, Ler LW, Sonenberg N. eIF4E–from translation to transformation. Oncogene. 2004;23(18):3172–9.

45. Li BD, McDonald JC, Nassar R, De Benedetti A. Clinical outcome in stage I to III breast carcinoma and eIF4E overexpression. Ann Surg. 1998;227(5):756–6. l; discussion 61 – 3.

Figures

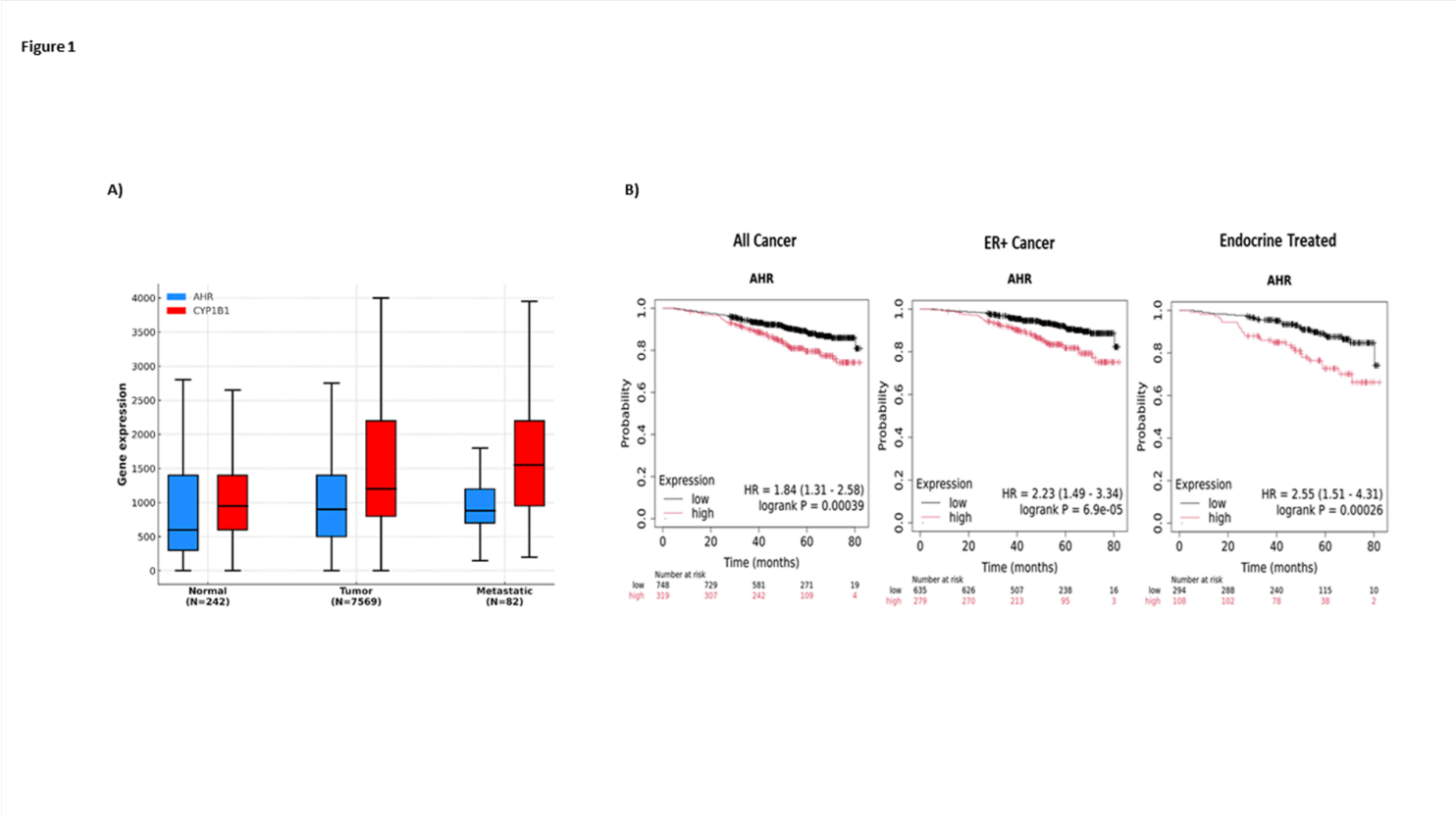


Figure 1

AhR gene expression and its predictive value in breast cancer patients. (A) Analysis with the TNMplot tool shows elevated AhR and CYP1B1 genes expression in tumor (P = 1.00e-06, Dunn's test) and metastatic (P = 1.83e-03, Dunn's test) for AhR in breast cancer tissues compared to normal breast tissues.(B) AhR overexpression correlates with reduced overall survival (OS) in breast cancer patients. Kaplan–Meier survival curves were generated using the Kaplan–Meier plotter to assess the impact of AhR mRNA expression on patient survival. Patients with AhR expression above the median are represented by the red line, and those below the median by the black line. HR indicates the hazard ratio. Statistical significance is shown with a p-value of 0.00017 for all breast cancer, p-value of 3.4e-5 for ER+ breast cancer, p-value of 8.1e-5 for endocrine treated, respectively.

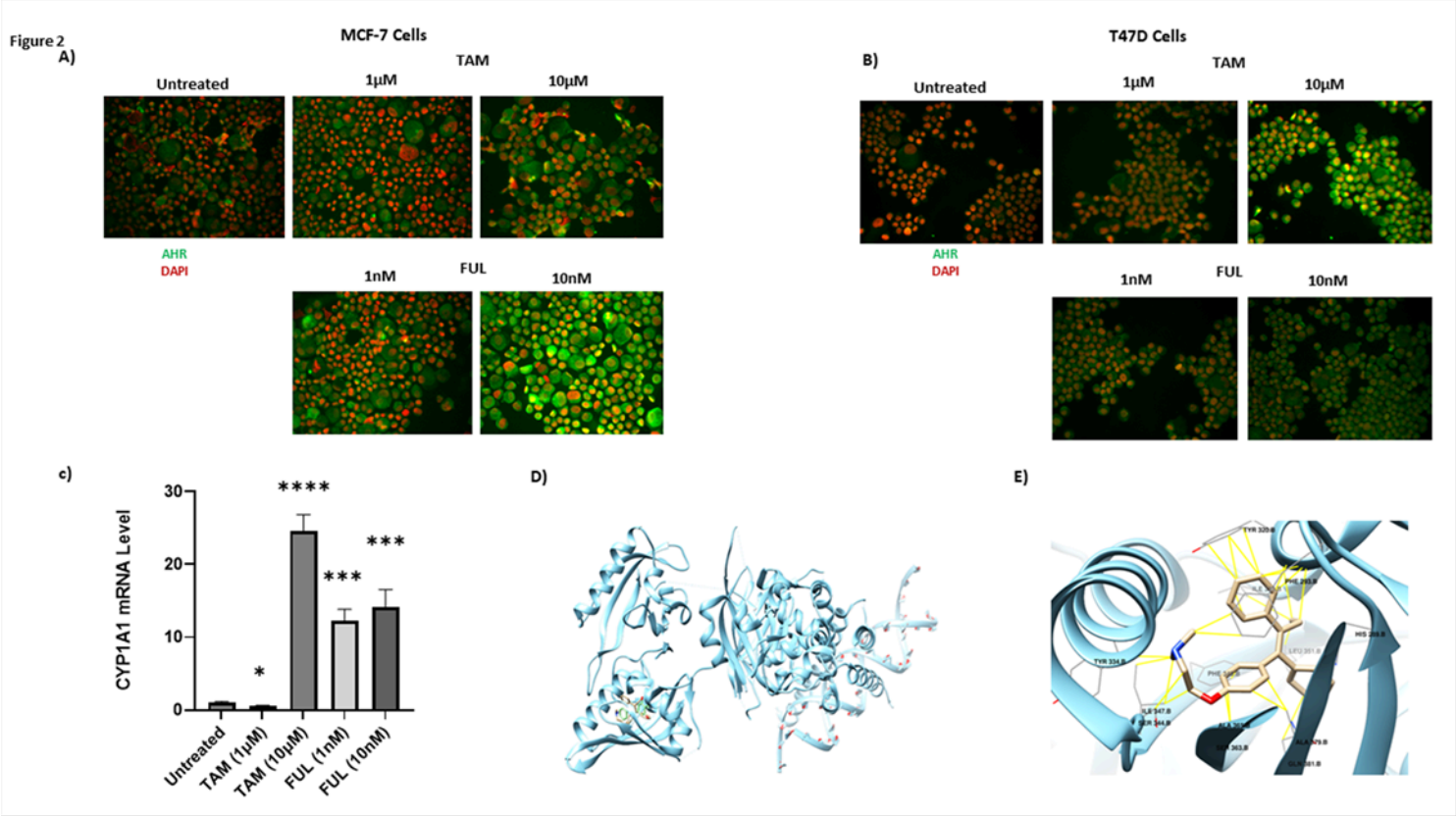


Figure 2

The endocrine therapeutic agents Tamoxifen and Fulvestrant activate AhR. (A) MCF-7 cells were treated with TAM 1 and 10 (μM) and FUL 1 and 10 (nM) for 48 hours. Cells were then stained with primary antibodies against AhR (green), followed by secondary antibodies and counterstained with DAPI (red). AhR protein localization was subsequently analyzed by immunofluorescence assay. (B) T47D cells were treated with TAM 1 and 10 (μM) and FUL 1 and 10 (nM) for 48 hours. AhR protein expression and localization were assessed by immunofluorescence assay. (C) mRNA expression levels of CYP1A1 were quantified by RT-PCR and normalized to the β-ACTIN housekeeping gene. Duplicate reactions were performed for each experiment, and data are presented as mean ± SEM (n = 6). Statistical significance compared to untreated cells was determined by Student's t-test: *P < 0.05; ***P < 0.001; ****P < 0.0001. (D) Binding conformations of tamoxifen (colored beige) and tapianrof (colored beige) at the binding site of ARH-ARNT heterodimer (pdb id: 8XS6). (E) Hydrophobic interactions (yellow colored lines) of TAM (beige colored stick) to the hydrophobic side chains of binding site's amino acid residues (colored by atom wire).

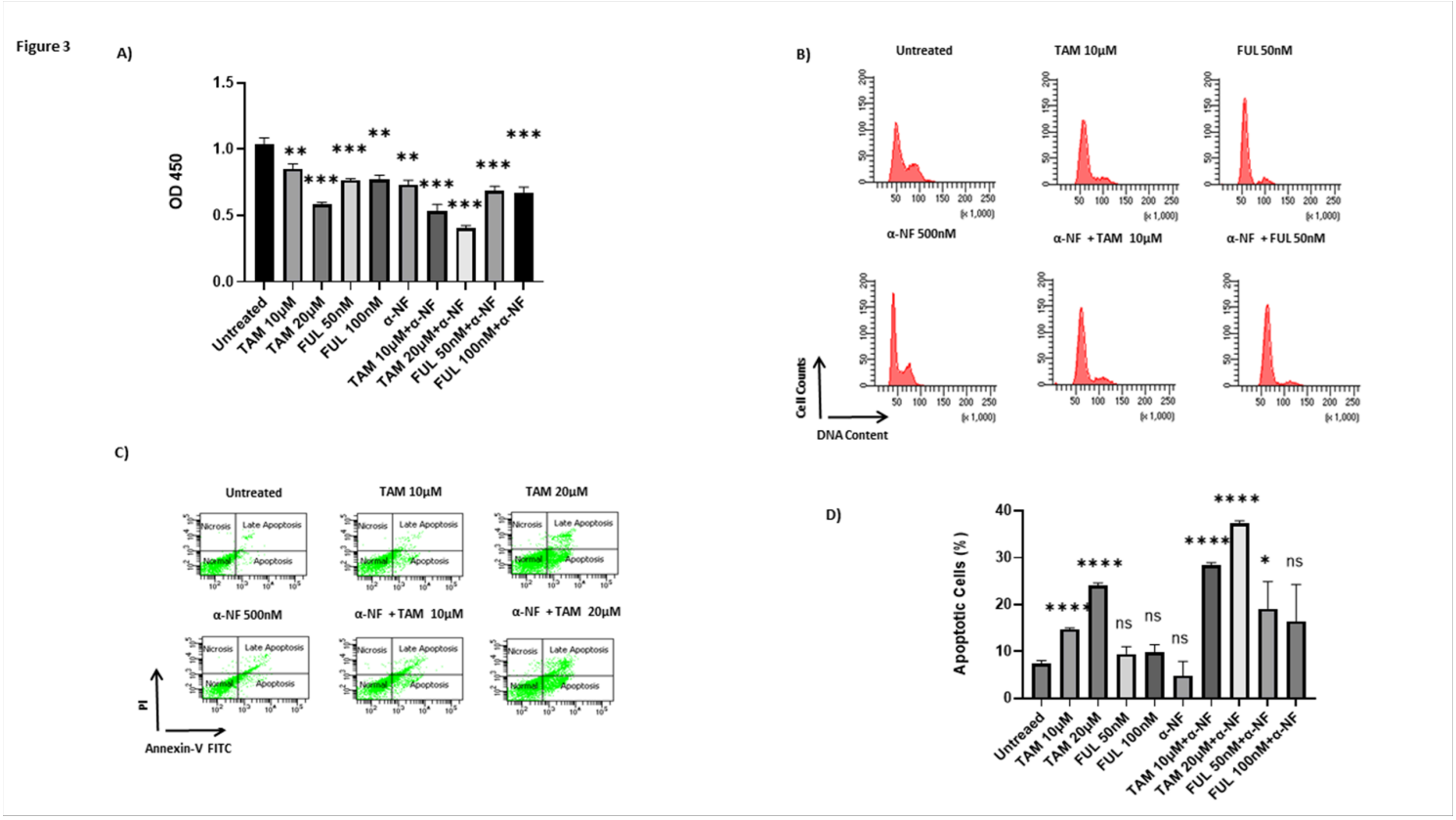


Figure 3

AhR inhibition increased therapeutic effect of Tamoxifen and Fulvestrant in breast cancer cells. (A) Optic density (OD) was quantified using xMark™ microplate absorbance spectrophotometer. Duplicate reactions were performed for each experiment and data are presented as mean ± SEM (n = 4). Statistical significance compared to untreated cells was determined by Student's t-test: **P < 0.01; ***P < 0.001. (B) Representative DNA fluorescence histograms of MCF-7 cells: untreated control, treated with TAM, FUL, and combined treatment with α-NF. (C) Representative dot plot of Annexin V and DAPI staining following treatment of MCF-7 cells with TAM and FUL alone or in combined treatment with α-NF. (D) Duplicate runs were performed for each experiment, and data are presented as mean ± SEM (n = 4). Percentage of cells that underwent apoptosis was analyzed on LSRII Flow Cytometer.

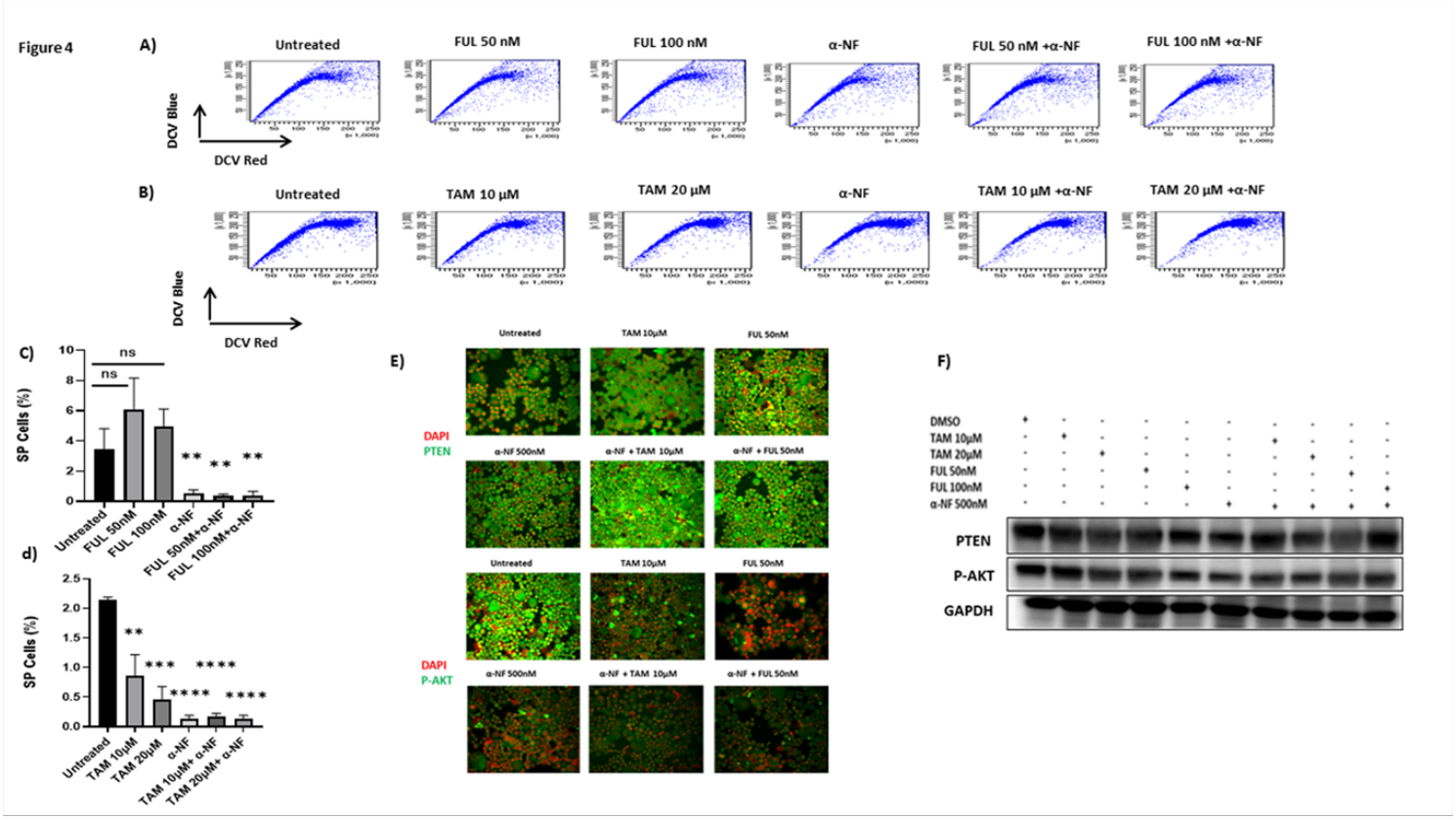


Figure 4

Inhibition of AhR enhances the reduction of side population (SP) cells induced by tamoxifen and fulvestrant treatment. (A) and (B) MCF-7 cells, either untreated or treated with TAM, FUL alone, or in combination with α-NF , were incubated with 10 (μM) DCV. The percentage of side population (SP) cells was thereafter measured using BD LSRFortessa™ flow cytometer. (C) and (D) Duplicate runs were performed for each experiment, and data are presented as mean ± SEM (n = 4). (E) MCF-7 cells treated as indicated were stained with primary antibodies against PTEN and phosphorylated AKT (P-AKT) (green), followed by secondary antibodies, and counterstained with DAPI (red).Protein expression and localization was analyzed by immunofluorescence microscopy. (F) Protein expression levels were assessed by Western blot analysis using the enhanced chemiluminescence method. A representative blot from duplicate experiments is shown.

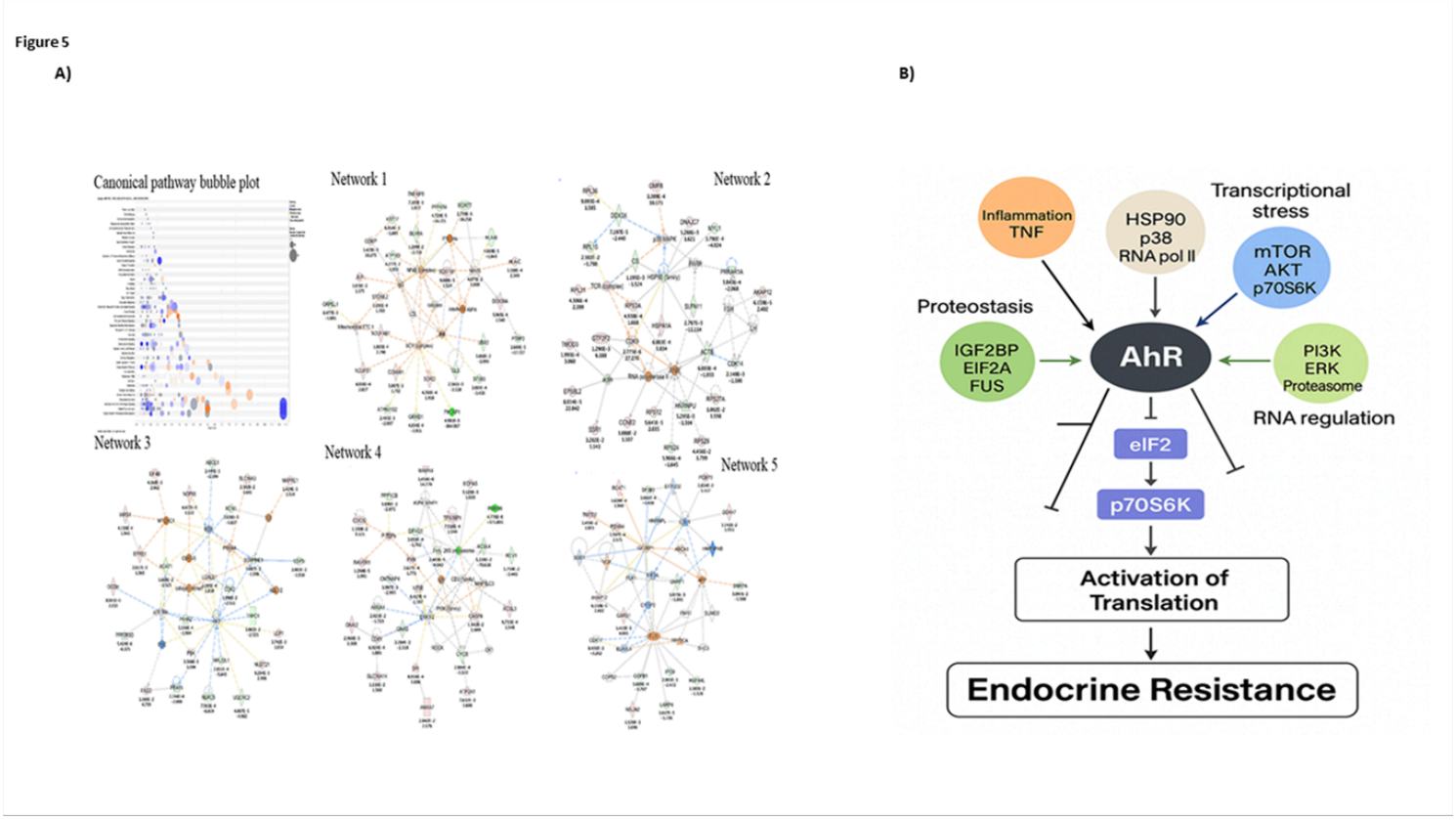


Figure 5

Integrated mechanistic model of AhR-mediated endocrine therapy resistance via translational activation. (A) Proteomic pathway analysis revealed five major signaling networks that converge on a unified resistance program. Network 1 centered on MAPK, JNK, and AKT activation, integrating acute-phase proteins (SAA, CRP, LBP) and complement/coagulation factors (F2, FGA/B/G, C4B, CFHR1). This module reflects tissue damage–induced inflammatory and coagulation responses driving survival signaling. Network 3 linked VEGF–ERK–PI3K signaling with complement components (C1R, C1S, C4A, CFB) and the NF-κB complex, representing pro-angiogenic and innate immune crosstalk characteristic of hypoxic and remodeling microenvironments. Network 4 was dominated by NF-κB (RELA) and transcriptional regulators (SOX2, SP1, EHF), connecting chemokine expression (CXCL16, CCL18), acute-phase reactants, and complement control proteins (CFH). This network defines a chronic inflammatory and stemness-promoting signaling hub. Network 5 encompassed HIF-1α, EGFR, mTOR, and β-catenin (CTNNB1) modules, indicating hypoxia-driven metabolic adaptation and EMT pathways that reinforce resistance. (B) Schematic summarizes the major molecular interactions linking AhR activation to translational reprogramming and therapy resistance identified through proteomic and IPA analyses.

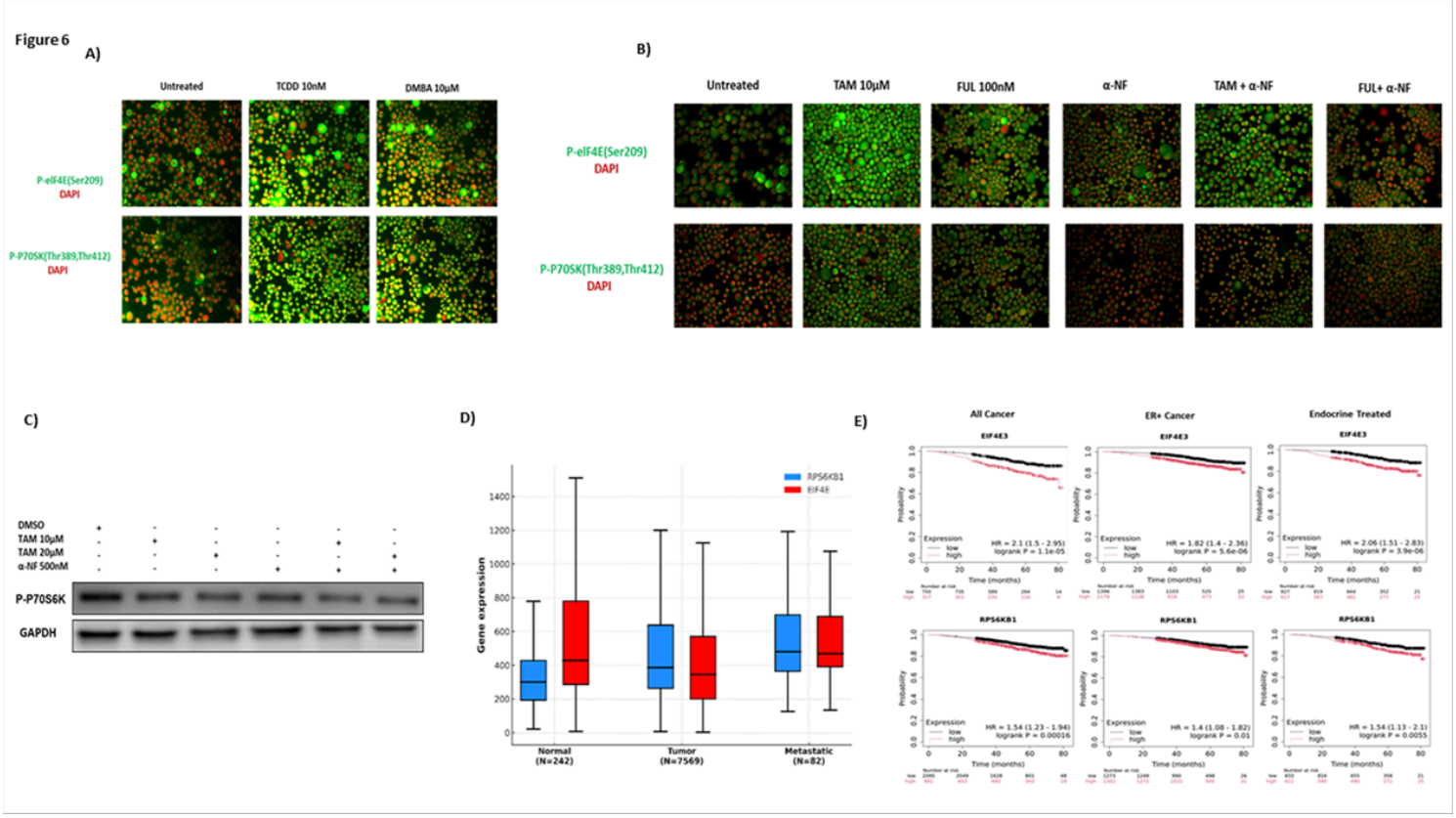


Figure 6

Activation of AhR enhances phosphorylation of eIF4 and p70S6K. (A) Enhanced phosphorylation of eIF4 and p70S6K in HMLE cells following TCDD and DMBA treatment, as demonstrated by immunofluorescence (IF) assay. (B) MCF-7 cells were pretreated with α-NF for 2hrs. Thereafter, cells were treated with TAM 10 (μM) and FUL 100 (nM) for 48 hours. Cells were then stained with primary antibodies against p-eIF4 and p-p70S6K (green), followed by secondary antibodies and counterstained with DAPI (red). AhR protein localization was subsequently analyzed by immunofluorescence assay. (C) Protein expression levels were assessed by Western blot analysis using the enhanced chemiluminescence method. A representative blot from duplicate experiments is shown. (D) Analysis of EIF4E3 and RPS6KB1 gene expression in normal, tumor and metastasis breast tissue using the TNMplot tool. (E) EIF4E3 and RPS6KB1 overexpression correlates with reduced overall survival in breast cancer patients. Kaplan–Meier survival curves were generated using the Kaplan–Meier plotter to assess the impact of EIF4E3 and RPS6KB1 mRNA expression on patient survival. Patients with gene expression above the median are represented by the red line, and those below the median by the black line. HR indicates the hazard ratio. Statistical long rank p-value is shown.

Supplementary Files

This is a list of supplementary files associated with this preprint. Click to download.

- S.Fig1.tif